An.D. ZOLOTARENKO [1,2,*], Ol.D. ZOLOTARENKO [1,2,**],
Z.A. MATYSINA [1], N.A. SHVACHKO [1,3], N.Y. AKHANOVA [4,5],
M. UALKHANOVA [5], D.V. SCHUR [1,6,***], M.T. GABDULLIN [4],
Yu.I. ZHIRKO [6], Yu.M. SOLONIN [1,****], V.V. LOBANOV [2],
D.V. ISMAILOV [5,7], A.D. ZOLOTARENKO [1], and I.V. ZAGORULKO [8,***]

[1] I.M. Frantsevych Institute for Problems of Materials Science of the N.A.S. of Ukraine,
   Omeljan Pritsak Str., UA-03142 Kyiv, Ukraine
[2] O.O. Chuiko Institute of Surface Chemistry of the N.A.S. of Ukraine,
   17 General Naumov Str., UA-03164 Kyiv, Ukraine
[3] Kyiv National University of Construction and Architecture,
   31 Povitroflotskyi Ave., UA-03037 Kyiv, Ukraine
[4] Kazakh–British Technical University,
   59 Tole bi Str., 050000 Almaty, Kazakhstan
[5] Al-Farabi Kazakh National University,
   71 Al-Farabi Ave., 050040 Almaty, Kazakhstan
[6] Institute of Applied Physics of the N.A.S. of Ukraine,
   58 Petropavlivska Str., UA-40000 Sumy, Ukraine
[7] NJSC 'K.I. Satbayev Kazakh National Research Technical University',
   22a Satbaev Str., 050013 Almaty, Kazakhstan
[8] G.V. Kurdyumov Institute for Metal Physics of the N.A.S. of Ukraine,
   36 Academician Vernadsky Blvd., UA-03142 Kyiv, Ukraine

* a.d.zolotarenko@gmail.com, ** o.d.zolotarenko@gmail.com,
*** dmitry.schur@gmail.com, **** solonin@ipms.kiev.ua

ON THE SOLUBILITY OF HYDROGEN IN METALS AND ALLOYS

We review and analyse the factors affecting the solubility of interstitial atoms (H) in the metal alloys. The electronic structure and atomic ordering of the AB-type alloys, as well as methods of calculation of the solubility for ordering cubic alloys

with octahedral interstitial pores are considered. We study the parameters of interstitial atoms, which make it possible to predict a decrease or increase in solubility, when the main role belongs to the ordering of the system. The parameters of the static distribution of atoms are determined. The relative solubility is represented as a function of the long-range order parameter (η), and the influence of bulk effects on this parameter is considered. The following systems are studied: Fe–Ni, Au–Cu, Pd–Au, Fe–Cr, Ti–Al, Cu–Zn, Ag–Zn, Fe–Al, Au–Ag, Fe–V, Pd–Pt, Ni–Mn, Ni–Fe, Cu–Au, Cu–Pd, Pd–Nb, Pd–Ag, as well as three-component alloys. As shown, through introducing impurities into the alloy, we can change significantly its physical-mechanical, electrical, magnetic, and other properties.

Keywords: metals, alloys, interstitial atoms, solubility, ordering, body-centred cubic (b.c.c.) structure, face-centred cubic (f.c.c.) structure, molecular kinetic theory.

1. Role of Impurities in the Properties' Modification

Solubility is one of the most important properties of metals and alloys. As known in reality, only solutions exist, and pure substances represent an ultimate state that can be approached. In many cases, it is necessary to have data on the maximum solubility of a specific element in a metal or alloy. This information allows us to determine the concentration range of the element within which it dissolves in the alloy without disrupting the homogeneity of the solid solution. By introducing impurities (alloying elements) into the alloy, we can significantly change its mechanical, electrical, magnetic, and other properties. Therefore, multicomponent solid solutions based on pure metals or binary alloys have great practical value and are known to be the main structural components of practically all used alloys.

There is already a significant amount of literature [1–27] describing the preparation [1–6] and processing [7–10] of metals and their alloys, as well as summarizing experimental [11–18] and theoretical [19–21] data on single-component [22–23] or multicomponent [24–27] systems. Studying these materials allows us to establish the nature of the influence of various impurities on the physical properties of metals or alloys. In addition, the available information allows us to consider metals and alloys as catalysts used to obtain a wide range of soluble (fullerenes [28–31], fullerites [32], endofullerenes [33]) and insoluble carbon nanostructures (graphene [34–35], nanotubes [36–37]) in various synthesis methods [38–46]. Such nanomaterials can be used in additive technologies [47–50], solar energy [51–53], as well as in the production of sorbents [54–62] in the medical-biological industry [63–68] and modern composite materials [69–72]. In addition, carbon nanostructures play an important role in hydrogen energy as materials for fuel cells [73–76] and hydrogen storage [77–81], where nanostructures compete with widely known advanced hydrogen storage materials [82–99].

From the beginning of studying solid solutions [100], it was found that impurities significantly affect the electrical properties of alloys. For example, the effect of gases dissolved in metals on their physical properties has been investigated. In most cases, gases increase the hardness and decrease the ductility of metallic materials, leading to brittleness [101, 102]. Thus, the failure of metallic products during operation is a consequence of the presence of gas impurities in them. In addition, the presence of Hydrogen (H_2) in an alloy can affect the processes of diffusion and atom ordering, as demonstrated in the case of Fe–Ni and Au–Cu alloy systems [103–106]. Hydrogen also changes the electrical resistance of alloys, *e.g.*, small amounts of hydrogen increased the resistance of the Pd–Au alloy [101]. The authors of Ref. [101] discovered a strong influence of gas on the thermoelectric power of metals.

Adding a third element to a binary alloy changes the phase diagram type. This circumstance should be taken into account [107], *e.g.*, for solving problems related to developing the heat treatment regimes for alloys, determining the possibility of metastable phases appearing, determining conditions for phase equilibrium, *etc*. In the case of ordering binary systems, adding a third element can expand or narrow the range of existence of the ordered phase. For example, adding V or Mo to Fe–Cr alloy increases the ordering temperature [108, 109], while adding Cr to Fe–V decreases this parameter [108]. Adding V or Nb to Ti–Al also reduces the ordering temperature, while increasing its heat resistance [110].

2. Factors Affecting the Solubility

Factors affecting the solubility of an element in a metal or alloy can be divided into external and internal. External factors affecting solubility depend on the conditions in which the system is located, *i.e.* on temperature, pressure. As shown in Ref. [111], the dependence of solubility S on temperature T is expressed by the equation

$$S = K_{\exp} - \frac{E_s}{k_B T},\qquad(1)$$

where K is a constant, E_s is the heat of dissolution, and k_B is the Boltzmann constant.

Figure 1 schematically shows the dependence of hydrogen solubility in different metals, where a is the melting point, b is the phase transformation point in iron. In liquid metals, the gas dissolves better; the solubility of hydrogen in solid aluminium (Al) is very low. As can be seen from Eq. (1), the dependence of the logarithm of solubility on the reciprocal temperature should be linear. The slope of this straight line can be used to determine the heat of dissolution.
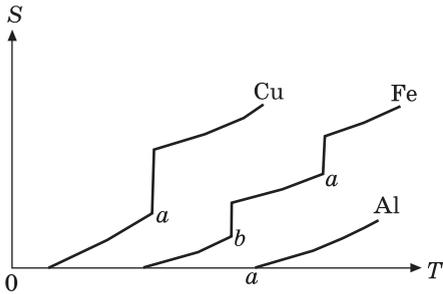
Fig. 1. Temperature dependence of hydrogen solubility in Cu, Fe and Al [111]

Gas usually dissolves in metals in small amounts, so that dissolved gas atoms do not interact with each other. In this case, solubility is proportional to pressure P, if the gas is monatomic, or proportional to $\sqrt{P}$, if the gas is diatomic, such as H_2 or C_2.

Internal factors affecting solubility can be divided into geometric, chemical, and physical factors, where:

• geometric factor is the different size of atoms;

• chemical factors of solubility are electronegativity and valence;

• physical factors of solubility are the structure of the alloy, quantitative ratio of components, and atomic order.

These factors affect not only solubility but also each other. The presence of impurity atoms deforms the crystal lattice, causing its compression or stretching and thereby changing the lattice period. If the alloy atoms differ only in size, then, the average atomic diameter and lattice parameter are determined by the Vegard's rule, which was derived for inorganic salts and solid solutions, but works well for Cu–Zn and Ag–Zn alloys. However, if the pure components differ in compressibility, valence, and electronegativity, then, the average atomic diameter and lattice parameter will not be a linear function of the alloy composition. The presence of atomic ordering in the alloy makes the concentration dependence of the lattice parameter complex, with kinks or breaks appearing on the graph of this dependence. The dependence of atomic diameter on the nearest neighbour arrangement was discovered in the work [121]. In the Fe–Al alloys, a superstructure manifests itself, when impurity atoms are dissolved in them, and the dependence of the lattice parameter on the composition in these alloys is complex. Disruption of the periodicity of the crystal lattice caused by impurity atoms is a serious obstacle to solubility. Atomic ordering promotes the restoration of lattice periodicity, resulting in a denser packing and a dec-rease in the lattice parameter. Therefore, often, the phenomena of ordering and good solubility accompany each other and have a mutual influence.

It has been experimentally established that the electronegativity of an element x is determined by its valence n and atomic radius r.

$$x \propto \frac{n+1}{r}.$$

Atoms with different valences (different electronegativity) have a greater affinity. This leads to an increase in the stability of the alloy and promotes atomic ordering.
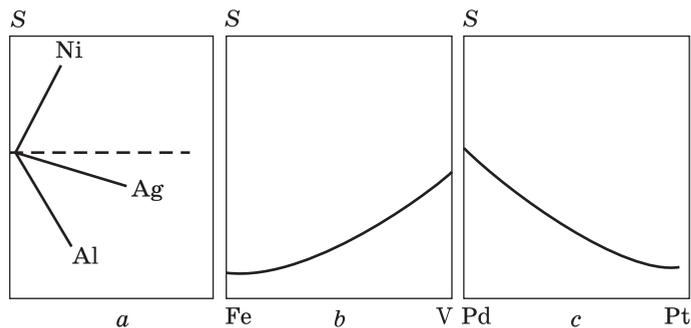
Fig. 2. Dependence of the solubility of hydrogen in a metal on the concentration of impurity metals [101]

Changes in the structure of the metal or alloy (phase transformation) cause a sharp change in solubility. Two elements form a continuous series of solid solutions if the crystal lattice of the solution is similar to the crystal lattices of the constituent elements. This is observed in the Au−Ag alloys.

Fig. 3. Temperature-dependent hydrogen solubility in Fe−V alloys [124, 125]

The solubility of gas in a metal is strongly influenced by the presence of impurities from other elements. If the metal is a good solvent, its impurities will increase solubility, and vice versa. Figure 2, *a* shows the dependence of hydrogen solubility in Cu on the content of Ni, Ag, or Al [101]. As seen from Figs. 2, *b* and 2, *c* showing the concentration dependence of hydrogen solubility in Fe−V and Pd−Pt alloys, respectively, the properties inherent to each specific metal are manifested (but not summed up) in the alloy. Impurity atoms affect the temperature dependence of solubility. For example, the temperature dependence of hydrogen solubility in iron-vanadium alloys is not determined by Eq. (1); a minimum is observed on the corresponding curve in the alloy with 22% vanadium at 900 °C (Fig. 3). However, despite the fact that, in most cases, there is an increase in the maximum solubility of components upon heating [124, 125], as Eq. (1) suggests, there are separate cases where the concentration range of solid solution narrows with increasing temperature of the alloy [108]. In these cases, phase transformations usually take place, where the effects of physical and chemical factors of dissolution should be taken into account.

To understand fully the mechanism of impurity dissolution, the electronic structure of the alloy must be taken into account. When an impurity atom enters a melt, it causes the appearance of a perturbing
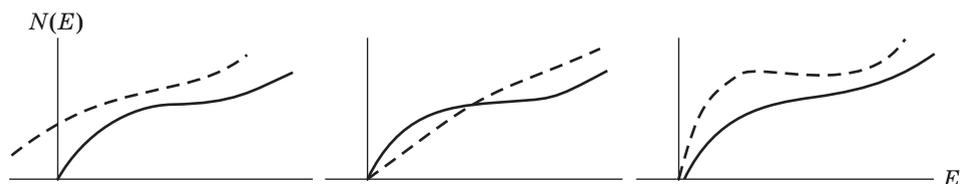
Fig. 4. Shifts in the density of state for different distributions of impurity atoms in the alloy, where dashed lines correspond to the random distributions [126]
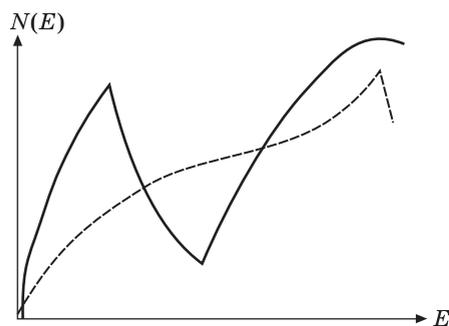
Fig. 5. Density of states of disordered (dashed line) and ordered (solid line) solid solutions [127]

field, altering the interaction between alloy atoms. This affects the distribution of electrons in bands according to energy levels and the density of states $N(E)$. If the distribution of impurity atoms in the alloy is disordered, there is a slight shift in the $N(E)$ curve as shown (by the dashed line) in Fig. 4 [126].

If a superstructure manifests in the alloy, there may be a split in the energy band. Figure 5 schematically shows the dependences $N(E)$ for disordered (dashed line) and ordered (solid line) solid solutions [127]. The presence of impurity atoms can cause the appearance of electronic irregularities and disrupt the periodicity of the distribution of electron charges in the crystal. This one results in the structural distortions, namely, displacement of atoms from equilibrium positions [128]. Such distortions (in turn) affect the solubility of impurities and the final properties of solid solutions. The consistent theory of solubility should take into account the electronic states of solid solutions.

3. Brief Theoretical Background for Studying the Solubility

To construct a theory of solubility, certain model representations are typically used. The model is considered better if its predictions are more accurate and in agreement with experimental observations. Usually, not all factors influencing the properties of alloys are taken into account in proposed models. The developed approximation can be considered correct if the influence of the unaccounted factors is weak. For this reason, molecular kinetic representations are often used in constructing theories of solid solutions.

Theoretical studies of some physical properties of alloys (including solubility) can be conducted without considering electronic states. Molecular kinetic theory (MKT) is constructed taking into account the

distribution, movement, and interaction of atoms using statistical physics methods with the application of thermodynamic functions.

Impurity atoms, depending on their sizes, can be located in the crystal-lattice sites or interstices. Therefore, substitutional and interstitial solid solutions are distinguished. Alloys of different metals represent substitutional solid solutions.

The dissolution of hydrogen, carbon, boron, nitrogen, and other elements with small atomic radii leads to the formation of interstitial solid solutions. As shown in Ref. [129], the atomic radius of the interstitial component must satisfy the condition

$$r_{\text{in}} < 0.59\,r, \tag{2}$$

where r is the average atomic radius of the alloy in which the impurity is dissolved.

In this case, the coordination of the interstitial atoms will be octahedral (6 nearest neighbouring atoms), if $0.41r < r_{\text{in}} < 0.59r$, and tetrahedral (4 nearest neighbouring atoms), if $r_{\text{in}} < 0.41r$.

Examples of interstitial alloys include ordered Pd–Pt, Fe–V, Ni–Mn, Ni–Fe, Cu–Au, and Cu–Pd alloys with hydrogen interstitial atoms. In the Pd–Nb, Pd–Ag, Cu–Au, and Cu–Pd alloys with hydrogen, short-range ordering of atoms can occur at high temperatures. Alloys based on V, Ti, Zn, and Nb with W or Mo can contain a large amount of interstitial C atoms, since they are formed as a result of mutual dissolution of so-called interstitial phases [129].

Impurity atoms come in a metal or alloy from another additive phase. The calculation of the solubility of impurity atoms is carried out assuming that the system is in a state of thermodynamic equilibrium. This can be either an alloy (metal) in equilibrium with a solid phase as the source of dissolved atoms, or a solid solution (metal) in a state of thermodynamic equilibrium with a coexisting gas phase. The condition for the equilibrium of two phases is the equality of temperatures, pressures, and chemical potentials.

The concentration of impurity atoms can be easily estimated if the impurity atoms in the alloy are located in interstices. In this case, the state function of the alloy is written as

$$Z = \sum_n \exp\frac{-E_n}{k_B T} = \sum_\kappa \exp\frac{-E_\kappa}{k_B T} \sum_T \exp\frac{-E_T}{k_B T}, \tag{3}$$

where $E_n = E_\kappa + E_T$ is the energy of the system in the n-th state. It consists of the configurational energy (E_κ) and the energy of thermal vibrations and electronic states (E_T). Adding an impurity atom to the structure changes the energy of the alloy. The configurational energy E_κ increases by μ (chemical potential), and the energy E_T increases by ν. The transfer of a C atom from the second phase to the AB alloy requires

energy expenditure,

$$u_i = -iA - (z - i)B, \tag{4}$$

determined by the sum of the energies of pair-wise interaction of the embedded C atom with the nearest A and B atoms in the alloy. In the last formula (4), $A = V_{AC}$ and $B = V_{BC}$ are interaction energies of atoms taken with opposite signs, z is the number of nearest neighbouring sites of the C atom in the alloy, of which i sites are occupied by A atoms and $z - i$ sites are occupied by B atoms. The difference $u_i - \mu - \nu$ determines the potential field, in which C atoms are distributed. Since only one C atom can enter each interstice, the distribution function of C atoms in interstices should be determined and described by a Fermi-type function. At low concentrations of C atoms, the Boltzmann distribution function can be used [130]. Then, the number of C atoms located in the i-th interstice will be equal to

$$n_i = N_i \exp \frac{-(u_i - \mu - \nu)}{k_B T}, \tag{5}$$

where N_i is the number of interstices in the alloy of type i (the i-th interstice is determined by the number of A atoms in the nearest sites). The total number of C atoms dissolved in the alloy is obtained by summing (5) over i:

$$n = \sum_i n_i = \lambda \upsilon \sum_i N_i \exp \frac{-u_i}{k_B T}, \tag{6}$$

where

$$\lambda = \exp \frac{\mu}{k_B T} \tag{7}$$

is the absolute activity, and

$$\upsilon = \exp \frac{\nu}{k_B T} \tag{8}$$

is a multiplier by which the vibrational part of the state function (formula (3)) increases upon embedding the C atom.

Calculation of the sum in Eq. (6) for an unordered alloy leads to the following result:

$$n_0 = \frac{m \lambda \upsilon}{a^3} \left(c_A e^{\frac{A}{k_B T}} + c_B e^{\frac{B}{k_B T}} \right)^z, \tag{9}$$

where m is the number of interstitial sites in the crystal lattice of the alloy, a is the lattice parameter, c_A and c_B are the atomic concentrations of components A and B.

Formula (9) was derived in Ref. [131] for alloys with f.c.c. structures. This formula is valid for all alloys whose crystal lattice is such that all z nearest neighbours to the interstitial site are equidistant from it. This is also applicable for h.c.p. alloys. If the interstitial site is surrounded by nearest neighbours located at different distances from it,

then the energy required to transfer atom C from the second phase to the interstitial site, also determined by the sum of the energies of pair-wise interactions of atom C with nearest neighbours A and B, will also contain energies $A = V_{AC}$, $B = V_{BC}$, $a = \upsilon_{AC}$, $b = \upsilon_{BC}$, corresponding to different distances from the interstitial site to the nearest neighbours. Calculation of the number of impurity atoms dissolved in an unordered alloy with an f.c.c. structure [131] yields the result:

$$n_0 = \frac{m\lambda\upsilon}{a^3}\left(c_A e^{\frac{A}{k_B T}} + c_B e^{\frac{B}{k_B T}} \right)^l \left(c_A e^{\frac{a}{k_B T}} + c_B e^{\frac{b}{k_B T}} \right)^{z-l}, \tag{10}$$

where l and $z - l$ are the numbers of nearest neighbours corresponding to different distances.

From formulas (9) and (10), it can be seen that for a pure metal, such as A, when $c_A = 1$ and $c_B = 0$, these relationships reduce to a formula of type (1). However, for an alloy, the dependence of $\ln n$ on the inverse temperature $1/T$ will not be linear. In Eq. (9), it is close to linear only when $|A - B|/(k_B T) \ll 1$. If $|A - B|/(k_B T)$ is of the order of unity and the energy parameters A and B have opposite signs, then, a minimum may be observed on the curve of solubility *versus* temperature, as shown in Fig. 3. The dependence of solubility on composition is monotonic, as observed in experiments (Fig. 2).

The difference in pair-wise interaction energies of atoms $A–B$ can be estimated from the values of enthalpies of dissolution. Using the first law of thermodynamics, it can be easily shown that

$$\frac{A - B}{k_B} = \frac{\lambda_A - \lambda_B}{zR}, \tag{11}$$

where R is the gas constant. Knowing the enthalpies of dissolution λ_A and λ_B of atoms C in pure components A and B, one can estimate the energy parameter (11) that enters into Eq. (9) for solubility.

Atomic ordering in an alloy AB can both facilitate and hinder the dissolution of component C in it. The calculation of solubility for ordering alloys with an f.c.c. structure of type AB yields:

$$n = \frac{2\lambda\upsilon}{a^3}\left[\left(c_A + \frac{1}{2}\eta \right) e^{\frac{A}{k_B T}} + \left(c_B - \frac{1}{2}\eta \right) e^{\frac{B}{k_B T}} \right]^3 \times$$
$$\times \left[\left(c_A - \frac{1}{2}\eta \right) e^{\frac{A}{k_B T}} + \left(c_B + \frac{1}{2}\eta \right) e^{\frac{B}{k_B T}} \right]^3, \tag{12}$$

where η is the long-range order (LRO) parameter in the arrangement of atoms. Figure 6, *a* shows the dependence of relative solubility
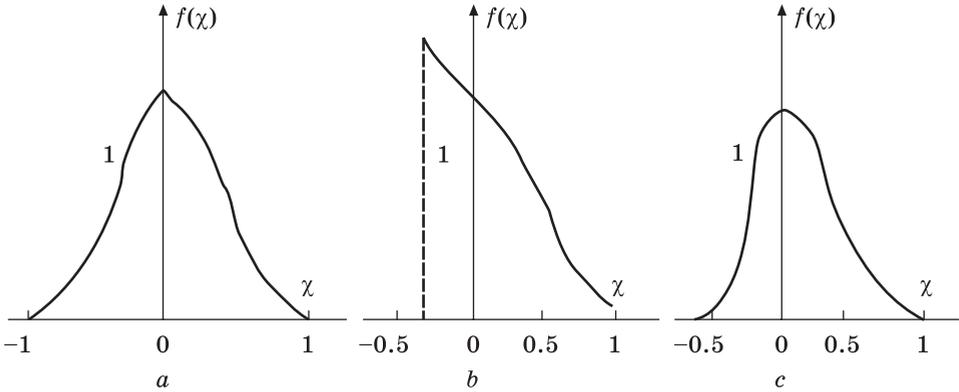
Fig. 6. Dependences of the relative solubility of interstitial atoms in the f.c.c. Cu_3Au-type alloy pores. Here, (*a*) solubility *vs.* parameter $\chi \propto \eta$, (*b*) and (*c*) octahedral and tetrahedral pores, respectively [131]

$$f = \frac{n}{n_0} = (1 - \chi^2)^3 \,, \tag{13}$$

where

$$\chi = \frac{1}{2} \eta \frac{e^{\frac{A}{k_B T}} - e^{\frac{A}{k_B T}}}{c_A e^{\frac{A}{k_B T}} + c_B e^{\frac{A}{k_B T}}} \,, \tag{14}$$

on the parameter χ, proportional to the LRO parameter η. Since $-1 \leq \chi \leq 1$, it can be seen from the graph that a higher ordering parameter leads to a decrease in the solubility of C atoms. As $\chi \to \pm 1$ (which can happen when $\eta \to 1$), solubility drops to zero, *i.e.*, in a fully ordered alloy, solubility is practically impossible. Therefore, to dissolve C atoms in an alloy (*e.g.*, to change its physical properties), it is necessary to reduce η and increase the temperature. As shown in Ref. [131], ordering can promote impurity solubility in alloys with f.c.c. and b.c.c. structures. This can be seen from Figs. 6 and 7 showing the dependence of relative solubility of atoms occupying octahedral (Fig. 6, *b*) and tetrahedral (Fig. 6, *c*) sites in f.c.c. Cu_3Au-type structure, and in octahedral sites of b.c.c. CuZn- (Fig. 7, *a*) and Fe_3Al-type structures (Fig. 7, *b*) on the parameter χ (or χ_1 and χ_2). The parameters χ_1 and χ_2 are determined by formulas like (14), but for χ_2 in (14), energies $A = V_{AC}$, $B = V_{BC}$ must be replaced by energies $a = \upsilon_{AC}$ and $b = \upsilon_{BC}$. For alloys with a b.c.c. lattice, the multiplier $1/2$ in this formula must be replaced by $1/4$. For such alloys, the value of χ can range from $[-1/3, 1]$; and in the range $[-1/3, 0]$, the solubility of impurity atoms in octahedral sites increases with increasing alloy ordering. For alloys with an f.c.c. structure, the
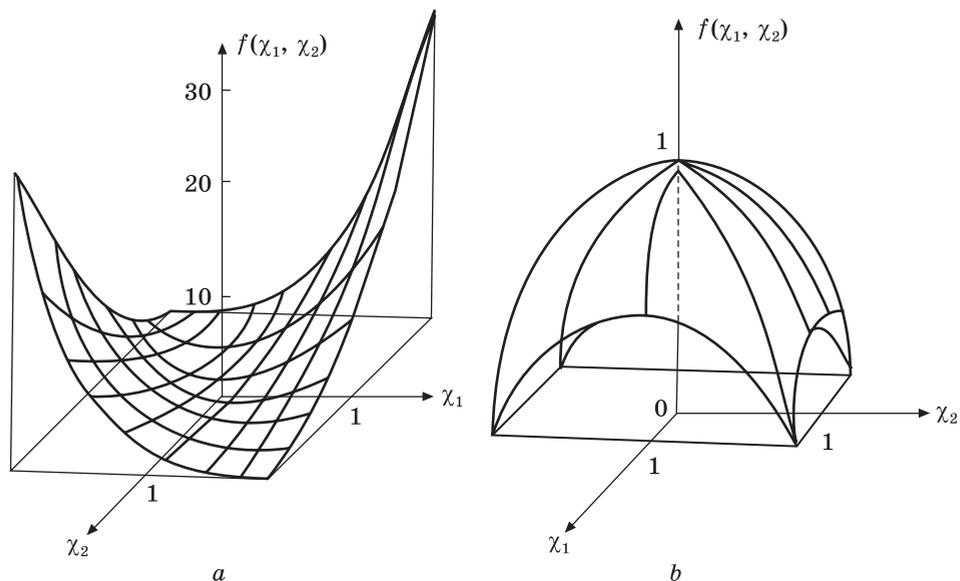
Fig. 7. Dependences of the relative solubility of atoms in the octahedral pores of the b.c.c. alloys, where *a* and *b* correspond to the CuZn- and Fe₃Al-type structures, respectively [131]

relative solubility is represented by the surface $f(\chi_1, \chi_2)$, and for alloys of CuZn type, ordering greatly increases solubility when χ_1 and χ_2 have opposite signs, *i.e.*, when the differences $A - B$ and $a - b$ are of opposite sign (this can happen if the potential curves $V_{AC}(r)$ and $V_{BC}(r)$ are significantly different).

In work [132], the concentration of dissolved C atoms in ordered AB alloys with an f.c.c. structure was determined for the case where the C atoms are located at the lattice sites:

$$c = \frac{\lambda \upsilon}{2}\left[\left(\frac{c_A + \frac{1}{2}\eta}{c_A - \frac{1}{2}\eta}\right)^{\frac{1}{2}} \exp\frac{8V_{AC} - 4V_{AA}}{kT} + \left(\frac{c_A - \frac{1}{2}\eta}{c_A + \frac{1}{2}\eta}\right)^{\frac{1}{2}} \exp\frac{8V_{AC} - 4V_{AA}}{kT}\right]. \quad (15)$$

Equation (15) indicates that the ordering of alloy atoms contributes to an increase in the solubility of C atoms. This can be explained by the redistribution of C atoms on the first and second type of lattice sites.

Formulas (9), (10), (12), and (15) are valid for a static distribution of atoms in the alloy. Additionally, in these formulas, the energies of pair-wise interatomic interactions are considered as constant. However, an analysis of typical ternary solid solutions shows that they cannot be considered as systems with a static distribution of atoms. The interac-
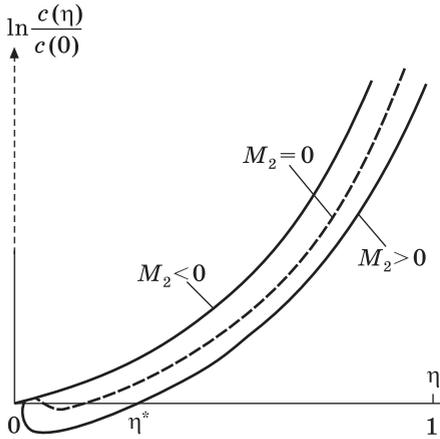
Fig. 8. Dependence of the concentration of dissolving impurity atoms on the LRO parameter (η) for substitutional b.c.c. alloys, where M_2 is an η-independent coefficient [148]

tion between alloy component atoms significantly influences the quantitative ratio of phases and, consequently, the overall construction of the ternary diagram [133]. As interatomic interaction depends on the alloy composition and order of atom placement on lattice sites, irregularities in the properties of continuous solid solutions occur with changes in their composition [134]. Among many classifications of binary and ternary metallic systems [100, 135−141, 142], conducted according to various criteria, such as the type of phase diagram, there is also a classification based on the nature of interatomic bonding [138].

These circumstances indicate the need to consider the dependence of interatomic interaction on composition and atomic order, when we study the impurity solubility in alloys.

In the works [143−145], authors studied the solubility in ordered substitutional and interstitial alloys taking into account the bulk effects. In papers [146, 147], the influence of comprehensive pressure on the solubility of a third component in binary ordered alloys was studied, which is important for understanding the process of impurity atom insertion into their crystalline lattice.

Bulk effects are taken into account by considering the dependence of atom interaction energies on the distance between them. In the literature, the energies of pair-wise atom interactions are often approximated by the widely used Lennard-Jones potential

$$V_{\alpha\beta}(r) = \frac{a_{\alpha\beta}}{r^m} - \frac{a'_{\alpha\beta}}{r^n}, \qquad m > n, \qquad \alpha, \ \beta = A, \ B, \ C, \qquad (16)$$

where m and n are positive integers, $a_{\alpha\beta}$, $a'_{\alpha\beta}$ are positive constants, the lattice parameter r changes with the composition c and ordering parameter η of the alloy and, in alloys under pressure, it also changes with pressure P. The dependence of $r(c, \eta)$ was determined [148−150] by minimizing the free energy F to achieve equilibrium in the alloy:

$$\frac{\partial F}{\partial r} = 0 . \qquad (17)$$

Calculations showed that for most alloys, the relative change in lat-

tice parameter $\omega = (r - r')/r'$ (r' is the average lattice parameter determined by Vegard's rule) can be both positive and negative, and its absolute value decreases with increasing atomic ordering parameter in the alloy. This has been confirmed experimentally. The dependence of interatomic distance on pressure was assumed to be linear [151–154]: $r = r_0(1 - lP)$, $lP \ll 1$, where r_0 is the distance between neighbouring atoms in the alloy at $P = 0$, and l is determined by the compressibility χ of the alloy $l = \chi/3$, $\chi = -(1/\upsilon)(\partial\upsilon/\partial P)$, υ is the volume of the alloy).

The influence of bulk effects and pressure on solubility largely depends on the potential curves $V_{\alpha\beta}(r)$, more precisely, on the values of parameters $a_{\alpha\beta}$, $a'_{\alpha\beta}$, m and n.

For the substitutional f.c.c. alloys, the concentration of dissolved impurity atoms is determined as in [148]:

$$c(\eta) = \lambda\upsilon(1 + \eta)^{-\frac{1}{2}}(1 - \eta)^{-\frac{1}{2}}\exp\frac{M_1 + M_2\omega(\eta)}{k_BT}, \qquad (17)$$

where M_1 and M_2 coefficients do not depend on η and are determined by parameters $a_{\alpha\beta}$, $a'_{\alpha\beta}$, m and n. When $M_2 = 0$, bulk effects in the alloy are absent. The last formula is written for an alloy of stoichiometric composition. Figure 8 shows graphs of the dependence of on η at $M_2 > 0$. When $M_2 > 0$ in the interval $[0, \eta^*]$, the ordering of the alloy components reduces the solubility of impurity atoms. However, as a rule, the solubility increases with increasing the LRO parameter.

Bulk effects lead to some characteristic features in the temperature dependence of solubility. As indicated in work [132], the curves of dependence of $\ln c(\eta)$ on $1/T$ have a kink at the temperature T_0 of the order−disorder phase transformation, if it is a second-order phase transition. Bulk effects can lead to the order-disorder transition being of the first order [148]. In this case, the function determining the dependence of $\ln c(\eta)$ on $1/T$ will experience a jump at T_0. The jump $\ln c(\eta_0) - \ln c(0)$, where $\eta_0 = \eta$ at $T = T_0$, will be positive.

The calculation of the solubility of impurity atoms shows that the graphs of relative solubility $f(\chi)$ or $f(\chi_1\chi_2)$ (Figs. 6 and 7) flatten out due to bulk effects. This means that the relative solubility as a function of the of LRO parameter in the arrangement of atoms decreases where it is greater than one, and increases where it is less than one. Therefore, with a constant LRO parameter, bulk effects smooth out the effect of changing (decreasing or increasing) solubility with ordering. However, investigation has shown that bulk effects strongly affect the LRO parameter in the alloy. Changing the lattice parameter of the crystal promotes greater ordering in the arrangement of atoms in the alloy. An estimate of the solubility of impurity atoms in alloys with an f.c.c. structure and octahedral interstitial sites showed that for positive values of the χ parameter, significant (more than twice) reduction in solu-

bility can occur due to bulk effects, and for negative χ, an increase of approximately 1.5 times can occur. This can explain the approximately two-fold increase in hydrogen solubility in Ni−Mn and Ni−Fe alloys [155] upon their ordering.

In the b.c.c.-lattice-based alloys, an interesting effect is possible. If there is a strong difference in the potential curves $V_{AC}(r)$ and $V_{BC}(r)$, the parameters $\chi_1(\eta)$ and $\chi_2(\eta)$ can vary due to the bulk effects such that instead of, *e.g.*, decreasing solubility with ordering (without considering bulk effects), we will actually observe an increase in solubility with ordering (when considering bulk effects).

4. Pressure Effect on the Solubility

When we study the effect of pressure on the solubility of impurity atoms in ordered alloys, it should be noted that pressure strongly affects the LRO in the alloy [151]. Figure 9 exhibits possible dependencies of $\eta = \eta(P)$ for substitution f.c.c. alloys of stoichiometric composition, whereas the nonstoichiometric structures have been considered in Ref. [156]. Under pressure, the LRO parameter can either decrease (Fig. 9, *a*) or increase (Fig. 9, *b*). At certain pressure values P_0 (ordering pressure), a phase transition from order to disorder can occur in such an alloy, and there may be two such points, one at which order disappears and another at which it appears. Figure 10 shows graphs of the dependence of solubility on pressure, where dashed curves correspond to the disordered alloy and solid curves correspond to the ordered alloy. The solubility in the disordered alloy increases or decreases with pressure, and the graphs of this dependence have extreme or not, which is determined by the values of the parameters $a_{\alpha\beta}$, $a'_{\alpha\beta}$, m, and n in Eq. (16) for the energies of pair-wise atomic interactions. That is the dependence of solubility on pressure is determined by the nature of the dependence of potential energies of atomic interactions on interatomic distance.

All these cases have been studied in works [146, 147, 156, 157] (see also a wide reference list in the review [157]). At ordering pressures P_0, kinks appear on the dependence curves of $c = c(P)$. For alloys with a b.c.c. lattice, jumps rather than kinks will be observed on the dependence curves of $c(P)$ at ordering pressures P_0. In addition, in the case of interstitial alloys with a b.c.c. host lattice, the nature of the dependence of $c(P)$ will be different for octahedral and tetrahedral interstitial sites [147].

In a detailed review [157] (see also references therein), the authors developed the statistical-thermodynamic model of f.c.c. substitutional alloys with both magnetic components as well as models of kinetics of a relaxation of both short-range [158−163] and long-range [164−170] atomic orders of alloys at zero pressure considered with use of the self-
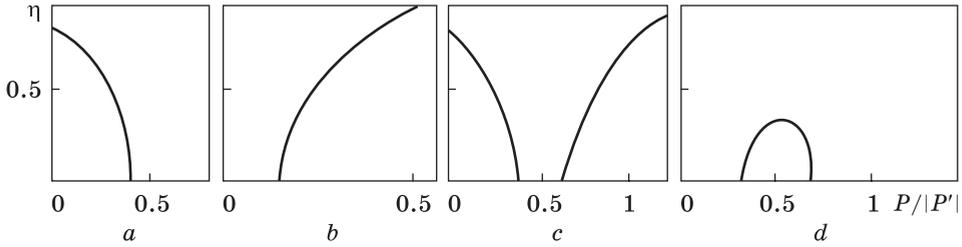
Fig. 9. The long-range order (LRO) parameter η *vs.* the reduced pressure, where η decreases (*a*), increases (*b*), decreases and then increases (*c*), increases and then decreases (*d*). In the last two cases (*c*, *d*), the order–disorder–order (*c*) and disorder–order–disorder (*d*) phase transformations occurs [146, 147, 151]
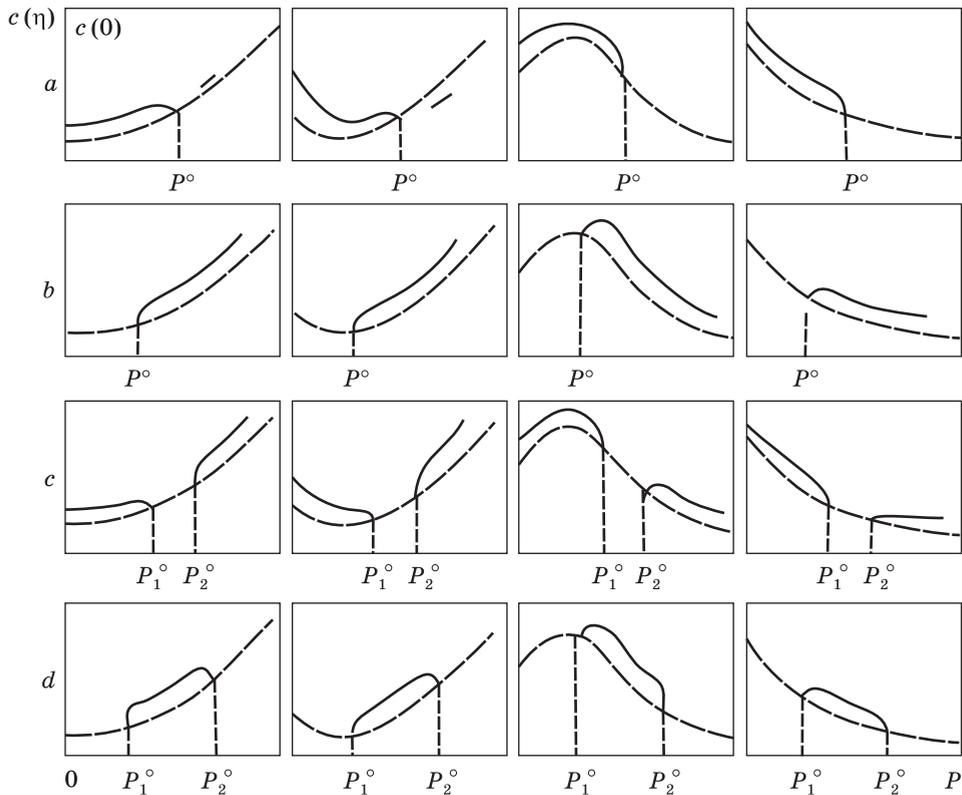
Fig. 10. Dependences of solubility ($c(\eta = 0)$ and $c(\eta \neq 0)$) on pressure (P) for disordered (dashed curves) and ordered (solid curves) alloys [146, 147, 151]

consistent field approximation. External pressure was taken into account in statistical-thermodynamic and kinetic models of f.c.c.-$L1_2$- or h.c.p.-$D0_{19}$-type orderings for two cases, namely, when dependences of volume of a sample of an alloy, V, on the LRO parameter, η, and com-

position are weak or essential, *i.e.*, when it is possible or it is impossible to neglect them, respectively. If this V weakly depends on η and composition, pressure P does not influence $\Delta\eta|_{T_0}$, *i.e.*, jump of the long-range order parameter. The pressure only displaces a point of the order–disorder phase transformation, T_0, aside high or low values of T, depending on signs of those parameters, which characterize model. The $T_0(P)$ and $\eta(P)$ dependences can be nonmonotonic, *i.e.*, occurrence of two different points of order–disorder phase transformations appears possibly. If V significantly depends on η and composition, $\Delta\eta|_{T_0}$ is not a constant and can increase or decrease with increase of P. Dependence $T_0(P)$ is almost linear or nonlinear at low or high values of P, respectively. The pressure can contribute to the atomic ordering or *vice versa* act against it, change a kind of phase transition and symmetry of a crystal lattice of an alloy because of its transformation from tetragonal structure into rhombohedral one [156, 157].

5. Summary

Through experimental investigation of the solubility of the third element in the binary ordered alloys, a number of practically important questions can be clarified. Since the solubility substantially depends on the type of interaction potentials between the alloyed and matrix atoms, an experimental study of the solubility will provide some information on the nature of the dependence $V_{AC} = V_{AC}(r)$ and $V_{BC} = V_{BC}(r)$, the ratio of the energies of V_{AC} and V_{BC}, and the dependence of these energies on the LRO parameter for different compositions.

Additionally, it can reveal information about the type of phase transition from order to disorder. By investigating the solubility of impurity atoms in alloys under pressure, one can determine the nature of the pair-wise atomic interaction energies and their dependence on pressure, as well as predict possible patterns of solubility dependence on pressure and changes in alloy properties under pressure. The effect of pressure on the ordering processes and interatomic interactions can also be used to predict the possible dependence of solubility on pressure for specific alloys. By investigating the solubility of impurity atoms in alloys subjected to pressure, one can find out, *e.g.*, what is the nature of the dependence of the energies of pair interaction of atoms (or some of their combinations): whether order–disorder phase transformations occur under such conditions, how many points of such transformations exist in the alloy, what is the value ordering pressure, into which pores (octahedral or tetrahedral) for interstitial alloys the atoms of the dissolved element fall, *etc*. If the nature of the effect of pressure on the ordering processes and on interatomic interaction is known, for each specific alloy, it is possible to predict the possible regularities in the dependence

of the solubility of impurity atoms and, consequently, to predict a possible change in the properties of alloys under pressure.

However, it should be borne in mind that the conducted studies of the influence of bulk effects and pressure on solubility are purely qualitative, primarily because such are the possibilities of molecular kinetic theory, and it is impossible to consider an alloy simply as a source of a potential field acting on an ensemble of atoms of a dissolving element. The impurity atoms modify this field, which, in turn, affects the processes of ordering of the alloy atoms. In addition, when refining the theory, it is necessary to take into account the correlation between the filling of lattice sites with atoms of different types, and the change in the environment of the interstitial atom in the alloy, and the local distortion of the crystal lattice around the interstitial atom, and the interaction of intervening atoms not only with the nearest neighbouring atoms, but also with atoms in the following coordination spheres, and, finally, the interaction of dissolved atoms with each other.

If we compare the calculated data with the results of experimental analysis, we should keep in mind the possibility of formation of antiphase domains in the alloy, as well as various phases in terms of the content of dissolved atoms (arising due to the manifestation of interaction between dissolved atoms), which will differ not only in the concentration of dissolved atoms, but also in the value of the lattice parameter and the order parameter. The presence of the latter significantly increases the solubility of impurity atoms. In addition, the results presented in the article are valid for alloys in which ordering reduces the lattice parameter. However, one cannot exclude the possibility of an increase in the lattice parameter with ordering, which will change the nature of the influence of volume effects and confining pressure on solubility in ordering alloys.

6. Conclusions

A review of a wide range of metals and alloys allows us to claim that the knowledge of the impurity solubility parameters makes it possible in the future to evaluate and predict many physical characteristics of multicomponent alloys. In this respect, currently we can conclude as follows below.

Atomic ordering in the AB alloy can either promote the dissolution of the interstitial C component in it or hinder its dissolution. Formulas are given for determining the solubility of impurity atoms in ordering alloys with an h.c.p. AB structure.

Ordering reduces the solubility of interstitial C atoms to zero for alloy AB at the parameter $\chi \to \pm 1$ (this can be at the LRO parameter $\eta \to 1$). That is, in a completely ordered alloy, solubility is difficult,

therefore, in order to dissolve C atoms in the AB alloy, it is necessary to reduce η and increase the temperature of the alloy.

In alloys of the CuZn type, the solubility increases strongly with increasing ordering of the system.

Formula (15) indicates that ordering contributes to an increase in the solubility of C atoms, which can be explained by the redistribution of C atoms on sites of the first and second types.

It has been established that formulas (9), (10), (12), and (15) are valid for a static distribution of atoms in the alloy. In addition, in these formulas, the energies of the pair-wise interaction of atoms are considered as constant.

Analysis of typical ternary solid solutions shows that they cannot be considered as systems with a static distribution of atoms. For such solid solutions, the interaction of the atoms of the alloy components has a significant effect on the quantitative ratio of the phases and, as a consequence, on the overall construction of the ternary diagram.

It is necessary to take into account the dependence of interatomic interaction on the composition and atomic order when studying the solubility of impurities in alloys.

Relative solubility, as a function of the LRO parameter (η), decreases where it is greater than one (>1) and increases where it is less than one (<1).

It has been established that volume effects greatly change the value of the LRO parameter (η) in the alloy.

A study of the solubility of impurity atoms in alloys with an f.c.c. structure and octahedral interstitial pores showed that at positive values of the parameter χ, due to volume effects, a significant decrease (more than two times) in solubility can occur, and at negative χ, an increase by about one and a half times. This can explain the increase in the ordering parameter in Ni−Mn and Ni−Fe alloys with increasing hydrogen solubility.

If the nature of the effect of pressure on the processes of ordering and on interatomic interaction is known for each specific alloy, it is possible to predict the possible patterns of the dependence of solubility and, therefore, to predict a possible change in the properties of alloys under pressure.

It is impossible to consider an alloy simply as a source of potential field acting on an ensemble of atoms of a dissolving element, since the dissolving atoms modify this field, which, in turn, affects the processes of ordering of the alloy atoms.

When we study the process of introducing of impurity atoms, it is necessary to take into account many factors. These are the correlation between the filling of lattice sites with atoms of different types, the change in the environment of the implanted atom in the alloy, the local

distortion of the crystal lattice around the implanted atom, the interaction of the implanted atoms not only with the nearest neighbouring atoms, but also with atoms in the following coordination spheres, and, finally, the interaction of dissolved atoms with each other.

The considered structures of the *AB* type can be used as a working fluid in hydrogen-based accumulators, which will make it possible to safely store and transport H for hydrogen energy.

REFERENCES

1. G.A. Baglyuk, O.M. Ivasyshyn, O.O. Stasyuk, and D.G. Savvakin, The effect of charge component composition on the structure and properties of titanium matrix sintered composites with high-modulus compounds, *Powder Metall. Met. Ceram.*, **56**: 45 (2017);
https://doi.org/10.1007/s11106-017-9870-z
2. D.N. Brodnikovskii, N.I. Lugovoi, N.P. Brodnikovskii, V.N. Slyunyaev, N.N. Kuz'menko, A.D. Vasil'ev, and S.A. Firstov, Powder metallurgy production of Ti–5.4 wt.% Si alloy. I. Simulating the formation of powder particles by centrifugal atomization, *Powder Metall. Met. Ceram.*, **52**: 409 (2013);
https://doi.org/10.1007/s11106-013-9541-7
3. K.A. Abdullin, M.T. Gabdullin, L.V. Gritsenko, D.V. Ismailov, Z.K. Kalkozova, S.E. Kumekov, Z.O. Mukash, A.Y. Sazonov, and E.I. Terukov, Electrical, optical, and photoluminescence properties of ZnO films subjected to thermal annealing and treatment in hydrogen plasma, *Semiconductors*, **50**, No. 8: 1010 (2016);
https://doi.org/10.1134/S1063782616080029
4. G.A. Baglyuk, L.A. Sosnovskii, and V.I. Volfman, Effect of carbon content on the properties of sintered steels doped with manganese and copper, *Powder Metall. Met. Ceram.*, **50**: 189 (2011);
https://doi.org/10.1007/s11106-011-9317-x
5. Y. Matvienko, A. Rud, S. Polishchuk, Y. Zagorodniy, N. Rud, and V. Trachevski, Effect of graphite additives on solid-state reactions in eutectic Al–Cu powder mixtures during high-energy ball milling, *Appl. Nanosci.*, **10**, No. 8: 2803 (2020);
https://doi.org/10.1007/s13204-019-01086-2
6. G.A. Baglyuk, A.I. Tolochin, A.V. Tolochina, R.V. Yakovenko, A.N. Gripachevckii, and M.E. Golovkova, Effect of process conditions on the structure and properties of the hot-forged fe3al intermetallic alloy, *Powder Metall. Met. Ceram.*, **55**: 297 (2016);
https://doi.org/10.1007/s11106-016-9805-0
7. O.O. Havryliuk and O.Y. Semchuk, Formation of periodic structures on the solid surface under laser irradiation, *Ukr. J. Phys.*, **62**, No. 1: 20 (2017);
https://doi.org/10.15407/ujpe62.01.0020
8. E.V. Khomenko, G.A. Baglyuk, and R.V. Minakova, Effect of deformation processing on the properties of Cu–50% Cr composite, *Powder Metal. Met. Ceram.*, **48**: 211 (2009);
https://doi.org/10.1007/s11106-009-9108-9
9. A.V. Mostovshchikov, A.P. Ilyin, I.K. Zabrodina, L.O. Root, and D.V. Ismailov, Measuring the changes in copper nanopowder conductivity during heating as a method for diagnosing its thermal stability, *Key Engineering Materials*, **769**: 146 (2018);

https://doi.org/10.4028/www.scientific.net/KEM.769.146

10. O.N. Sizonenko, G.A. Baglyuk, E.I. Taftai, A.D. Zaichenko, E.V. Lipyan, A.S. Torpakov, A.A. Zhdanov, and N.S. Pristash, Dispersion and carburization of titanium powders by electric discharge, *Powder Metall. Met. Ceram.*, **52**: 247 (2013);
https://doi.org/10.1007/s11106-013-9520-z

11. G.A. Baglyuk, S.G. Napara-Volgina, V.I. Vol'fman, A.A. Mamonova, and S.G. Pyatachuk, Thermal synthesis of Fe−B4C powder master alloys, *Powder Metall. Met. Ceram.*, **48**: 381 (2009);
https://doi.org/10.1007/s11106-009-9156-1

12. V.M. Gun'ko, V.V. Turov, E.M. Pakhlov, A.K. Matkovsky, T.V. Krupska, M.T. Kartel, and B. Charmas, Blends of amorphous/crystalline nanoalumina and hydrophobic amorphous nanosilica, *J. Non-Cryst. Sol.*, **500**: 351 (2018);
https://doi.org/10.1016/j.jnoncrysol.2018.08.020

13. I. Brodnikovska, L. Khomenkova, N. Korsunska, Yu. Polishchuk, M. Brychevskyi, Ye. Brodnikovskyi, D. Brodnikovskyi, I. Polishko, and O. Vasylyev, he investigation of 10Sc1CeSZ structure transformation and ionic conductivity, *Mater. Today: Proc.*, **50**, Pt. 4: 487 (2022);
https://doi.org/10.1016/j.matpr.2021.11.299

14. A.A. Biliuk, O.Y. Semchuk, and O.O. Havryliuk, Width of the surface plasmon resonance line in spherical metal nanoparticles, *Semicond. Phys., Quantum Electron. Optoelectron.*, **23**, No. 3: 308 (2020);
https://doi.org/10.15407/spqeo23.03.308

15. G.A. Baglyuk, V.N. Terekhov, and Y.F. Ternovoi, Structure and properties of powder austenitic die steels, *Powder Metall. Met. Ceram.*, **45**: 317 (2006);
https://doi.org/10.1007/s11106-006-0083-0

16. I. Brodnikovska, N. Korsunska, L. Khomenkova, Yu. Polishchuk, S. Lavoryk, M. Brychevskyi, Y. Brodnikovskyi, and O. Vasylyev, Grains, grain boundaries and total ionic conductivity of 10Sc1CeSZ and 8YSZ solid electrolytes affected by crystalline structure and dopant content, *Mater. Today: Proc.*, **6**, Pt. 2: 79 (2019);
https://doi.org/10.1016/j.matpr.2018.10.078

17. N. Nastasiienko, B. Palianytsia, M. Kartel, M. Larsson, and T. Kulik, Thermal transformation of caffeic acid on the nanoceria surface studied by temperature programmed desorption mass-spectrometry, thermogravimetric analysis and FT−IR spectroscopy, *Colloids Interfaces*, **3**, No. 1: 34 (2019);
https://doi.org/10.3390/colloids3010034

18. O.I. Tolochyn, G.A. Baglyuk, O.V. Tolochyna, Y.I. Evych, Y.M. Podrezov, and H.M. Molchanovska, Structure and physicomechanical properties of the Fe3Al intermetallic compound obtained by impact hot compaction, *Mater. Sci.*, **56**: 499 (2021);
https://doi.org/10.1007/s11003-021-00456-y

19. O.Y. Semchuk, A.A. Biliuk, and O.O. Havryliuk, The kinetic theory of the width of surface plasmon resonance line in metal nanoparticles, *Springer Proc. Phys.*, **264**: 3 (2021);
https://doi.org/10.1007/978-3-030-74800-5_1

20. D.N. Brodnikovskii, N.I. Lugovoi, N.P. Brodnikovskii, V.N. Slyunyaev, L.D. Kulak, A.D. Vasil'ev, and S.A. Firstov, Powder metallurgy production of Ti−5.4 wt.% Si alloy. II. Structure and strength of the sintered material, *Powder Metall. Met. Ceram.*, **52**: 539 (2014);
https://doi.org/10.1007/s11106-014-9557-7

21. A.A Biliuk, O.Yu. Semchuk, and O.O. Havryliuk, Kinetic theory of absorption of ultrashort laser pulses by ensembles of metallic nanoparticles under conditions of surface plasmon resonance, *Chem., Phys. Technol. Surf.*, **13**, No. 2: 190 (2022);
https://doi.org/10.15407/HFTP13.02.190

22. A.P. Ilyin, A.V. Mostovshchikov, L.O. Root, S.V. Zmanovskiy, D.V. Ismailov, and G.U. Ruzieva, *Bulletin of the Tomsk Polytechnic University, Geo Assets Engineering*, **330**, No. 8: 87 (2019) (in Russian);
https://doi.org/10.18799/24131830/2019/8/2215

23. L. Karachevtseva, M. Kartel, V. Kladko, O. Gudymenko, W. Bo, V. Bratus, O. Lytvynenko, V. Onyshchenko, and O. Stronska, Functionalization of 2D macroporous silicon under the high-pressure oxidation, *Appl. Surf. Sci.*, **434**: 142 (2018);
https://doi.org/10.1016/j.apsusc.2017.10.029

24. I. Brodnikovska, M. Brychevskyia, Y. Brodnikovskyi, D. Brodnikovskyi, O. Vasylyev, and A. Smirnova, Joint impedance spectroscopy and fractography data analysis of ceria doped scandia stabilized zirconia solid electrolyte modified by powder types and sintering temperature, *French-Ukr. J. Chem.*, **6**, No. 1: 128 (2018);
https://doi.org/10.17721/fujcV6I1P128-141

25. G.A. Baglyuk and L.A. Poznyak, The sintering of powder metallurgy high-speed steel with activating additions, *Powder Metall. Met. Ceram.*, **41**: 366 (2002);
https://doi.org/10.1023/A:1021113025628

26. D.N. Brodnikovsky, A.V. Golovash, S.V. Tkachenko, I.Yu. Okun, N.N. Kuz'menko, and S.A. Firstov, *Metallofiz. Noveishie Tekhnol.*, **28**: 165 (2006).

27. G.A. Baglyuk and L.A. Poznyak, *Poroshkovaya Metallurgiya* [Powder Metallurgy], Nos. 1−2: 34 (2001) (in Russian).

28. D.V. Schur, S.Y. Zaginaichenko, E.A. Lysenko, T.N. Golovchenko, and N.F. Javadov, The forming peculiarities of C_{60} molecule, *NATO Science for Peace and Security Series C: Environmental Security* (Eds. B. Baranowski, S.Y. Zaginaichenko, D.V. Schur, V.V. Skorokhod, and A. Veziroglu) (2008), p. 53;
https://doi.org/10.1007/978-1-4020-8898-8_5

29. Ol.D. Zolotarenko, O.P. Rudakova, N.E. Akhanova, An.D. Zolotarenko, D.V. Shchur, Z.A. Matysina, M.T. Gabdullin, M. Ualkhanova, N.A. Gavrilyuk, O.D. Zolotarenko, M.V. Chymbai, and I.V. Zagorulko, Comparative analysis of products of the fullerenes' and carbon-nanostructures' synthesis using the SIGE and FGDG-7 grades of graphite, *Nanosistemi, Nanomateriali, Nanotehnologii*, **20**, No. 3: 725 (2022);
https://doi.org/10.15407/nnn.20.03.725

30. V.M. Gun'ko, V.V. Turov, V.I. Zarko, G.P. Prykhod'ko, T.V. Krupska, A.P. Golovan, J. Skubiszewska-Zięba, B. Charmas, and M.T. Kartel, Unusual interfacial phenomena at a surface of fullerite and carbon nanotubes, *Chem. Phys.*, **459**: 172 (2015);
https://doi.org/10.1016/j.chemphys.2015.08.016

31. M.M. Nishchenko, S.P. Likhtorovich, A.G. Dubovoy, and T.A. Rashevskaya, Positron annihilation in C_{60} fullerites and fullerene-like nanovoids, *Carbon*, **41**, No. 7: 1381 (2003);
https://doi.org/10.1016/S0008-6223(03)00065-4

32. V.I. Lad'yanov, R.M. Nikonova, N.S. Larionova, V.V. Aksenova, V.V. Mukhgalin, and A.D. Rud', Deformation-induced changes in the structure of fullerites $C_{60/70}$ during their mechanical activation, *Phys. Solid State*, **55**: 1319 (2013);
https://doi.org/10.1134/S1063783413060206

33. Z.A. Matysina, Ol.D. Zolotarenko, O.P. Rudakova, N.Y. Akhanova, A.P. Po-
    mytkin, An.D. Zolotarenko, D.V. Shchur, M.T. Gabdullin, M. Ualkhanova,
    N.A. Gavrylyuk, A.D. Zolotarenko, M.V. Chymbai, and I.V. Zagorulko, Iron in
    Endometallofullerenes, *Prog. Phys. Met.*, **23**, No. 3: 510–527 (2022);
    https://doi.org/10.15407/ufm.23.03.510
34. M.T. Kartel, K.V. Voitko, Y.V. Grebelna, S.V. Zhuravskyi, K.O. Ivanenko,
    T.V. Kulyk, S.M. Makhno, and Y.I. Sementsov, Changes in the structure and
    properties of graphene oxide surfaces during reduction and modification,
    Chem., Phys. Technol. Surf., **13**, No. 2: 179 (2022);
    https://doi.org/10.15407/hftp13.02.179
35. A.D. Rud and I.M. Kiryan, Quantitative analysis of the local atomic structure
    in disordered carbon, *J. Non-Cryst. Sol.*, **386**: 1 (2014);
    https://doi.org/10.1016/j.jnoncrysol.2013.11.010
36. Yu.I. Sementsov, O.A. Cherniuk, S.V. Zhuravskyi, W. Bo, K.V. Voitko,
    O.M. Bakalinska, and M.T. Kartel, Synthesis and catalytic properties of nitro-
    gen-containing carbon nanotubes, *Chem., Phys. Technol. Surf.*, **12**, No. 2: 135
    (2021);
    https://doi.org/10.15407/hftp12.02.135
37. S. Barany, N. Kartel', and R. Meszaros, Electrokinetic potential of multilayer
    carbon nanotubes in aqueous solutions of electrolytes and surfactants, *Colloid
    J.*, **76**, No. 5: 509 (2014);
    https://doi.org/10.1134/S1061933X14050020
38. D.V. Schur, A.G. Dubovoy, S.Yu. Zaginaichenko, V.M. Adejev, A.V. Kotko,
    V.A. Bogolepov, A.F. Savenko, A.D. Zolotarenko, S.A. Firstov, and V.V. Sko-
    rokhod, Synthesis of carbon nanostructures in gaseous and liquid medium,
    NATO Security through Science Series A: Chemistry and Biology (Dordrecht:
    Springer: 2007), p. 199;
    https://doi.org/10.1007/978-1-4020-5514-0_25
39. S.Y. Zaginaichenko, D.V. Schur, and Z.A. Matysina, The peculiarities of carbon
    interaction with catalysts during the synthesis of carbon nanomaterials, *Carbon*,
    41, No. 7: 1349 (2003).
    https://doi.org/10.1016/S0008-6223(03)00059-9
40. L.Z. Boguslavskii, A.D. Rud', I.M. Kir'yan, N.S. Nazarova, and D.V. Vinnichenko,
    Properties of carbon nanomaterials produced from gaseous raw materials using
    high-frequency electrodischarge processing, *Surf. Engin. Appl. Electrochem.*, **51**,
    No. 2: 105 (2015);
    https://doi.org/10.3103/S1068375515020027
41. Z.A. Matysina, Ol.D. Zolotarenko, M. Ualkhanova, O.P. Rudakova, N.Y. Akhanova,
    An.D. Zolotarenko, D.V. Shchur, M.T. Gabdullin, N.A. Gavrylyuk, O.D. Zolotarenko,
    M.V. Chymbai, and I.V. Zagorulko, Electric arc methods to synthesize carbon
    nanostructures, *Prog. Phys. Met.*, **23**, No. 3: 528 (2022);
    https://doi.org/10.15407/ufm.23.03.528
42. O.M. Yakymchuk, O.M. Perepelytsina, A.D. Rud, I.M. Kirian, and M.V. Sydorenko,
    Impact of carbon nanomaterials on the formation of multicellular spheroids by
    tumor cells, *Phys. Status Solidi A*, **211**, No. 12: 2778 (2014);
    https://doi.org/10.1002/pssa.201431358
43. N.T. Kartel, N.V. Gerasimenko, N.N. Tsyba, A.D. Nikolaichuk, and G.A. Kov-
    tun, Synthesis and study of carbon sorbent prepared from polyethylene terephtha-
    late, *Rus. J. Appl. Chem.*, **74**, No. 10: 1765 (2001);
    https://doi.org/10.1023/A:1014894211046
44. Ol.D. Zolotarenko, M.N. Ualkhanova, E.P. Rudakova, N.Y. Akhanova, An.D. Zo-

lotarenko, D.V. Shchur, M.T. Gabdullin, N.A. Gavrylyuk, A.D. Zolotarenko, M.V. Chymbai, I.V. Zagorulko, and O.O. Havryliuk, Advantages and disadvantages of electric arc methods for the synthesis of carbon nanostructures, *Chem., Phys. Technol. Surf.*, **13**, No. 2: 209 (2022); https://doi.org/10.15407/hftp13.02.209

45. V.I. Oreshkin, S.A. Chaikovskii, N.A. Labetskaya, Y.F. Ivanov, K.V. Khishchenko, P.R. Levashov, N.I. Kuskova, and A.D. Rud', Phase transformations of carbon under extreme energy action, *Tech. Phys.*, **57**, No. 2: 198 (2012); https://doi.org/10.1134/S106378421202017X

46. A.D. Rud, A.M. Lakhnik, S.S. Mikhailova, O.V. Karban, D.V. Surnin, and F.Z. Gilmutdinov, Structure of Mg–C nanocomposites produced by mechanochemical synthesis, *J. Alloys Compd.*, **509**, Suppl. 2: S592 (2011); https://doi.org/10.1016/j.jallcom.2010.10.155

47. O.D. Zolotarenko, E.P. Rudakova, A.D. Zolotarenko, N.Y. Akhanova, M.N. Ualkhanova, D.V. Shchur, M.T. Gabdullin, N.A. Gavrylyuk, T.V. Myronenko, A.D. Zolotarenko, M.V. Chymbai, I.V. Zagorulko, Yu.O. Tarasenko, and O.O. Havryliuk, Platinum-containing carbon nanostructures for the creation of electrically conductive ceramics using 3D printing of CJP technology, *Chem., Phys. Technol. Surf.*, **13**, No. 3: 259 (2022); https://doi.org/10.15407/hftp13.03.259

48. Ol.D. Zolotarenko, E.P. Rudakova, N.Y. Akhanova, An.D. Zolotarenko, D.V. Shchur, M.T. Gabdullin, M. Ualkhanova, M. Sultangazina, N.A. Gavrylyuk, M.V. Chymbai, A.D. Zolotarenko, I.V. Zagorulko, and Yu.O. Tarasenko, Plasmochemical synthesis of platinum-containing carbon nanostructures suitable for CJP 3D-printing, *Metallofiz. Noveishie Tekhnol.*, **44**, No. 3: 343 (2022); https://doi.org/10.15407/mfint.44.03.0343

49. Ol.D. Zolotarenko, E.P. Rudakova, N.Y. Akhanova, An.D. Zolotarenko, D.V. Shchur, M.T. Gabdullin, M. Ualkhanova, N.A. Gavrylyuk, M.V. Chymbai, T.V. Myronenko, I.V. Zagorulko, A.D. Zolotarenko, and O.O. Havryliuk, Electrically conductive composites based on TiO_2 and carbon nanostructures manufactured using 3D printing of CJP technology, *Chem., Phys. Technol. Surf.*, **13**, No. 4: 415 (2022); https://doi.org/10.15407/hftp13.04.415

50. Ol.D. Zolotarenko, E.P. Rudakova, N.Y. Akhanova, An.D. Zolotarenko, D.V. Shchur, M.T. Gabdullin, M. Ualkhanova, N.A. Gavrylyuk, M.V. Chymbai, Yu.O. Tarasenko, I.V. Zagorulko, and A.D. Zolotarenko, Electric conductive composites based on metal oxides and carbon nanostructures, *Metallofiz. Noveishie Tekhnol.*, **43**, No. 10: 1417 (2021); https://doi.org/10.15407/mfint.43.10.1417

51. O. Pylypova, O. Havryliuk, S. Antonin, A. Evtukh, V. Skryshevsky, I. Ivanov, and S. Shmahlii, Influence of nanostructure geometry on light trapping in solar cells, *Appl. Nanosci.*, **12**, No. 3: 769 (2022); https://doi.org/10.1007/s13204-021-01699-6

52. O.Y. Semchuk, A.A. Biliuk, O.O. Havryliuk, and A.I. Biliuk, Kinetic theory of electroconductivity of metal nanoparticles in the condition of surface plasmon resonance, *Appl. Surf. Sci. Adv.*, **3**: 100057 (2021); https://doi.org/10.1016/j.apsadv.2021.100057

53. O.O. Havryliuk, A.A. Evtukh, O.V. Pylypova, O.Y. Semchuk, I.I. Ivanov, and V.F. Zabolotnyi, Plasmonic enhancement of light to improve the parameters of solar cells, *Appl. Nanosci.*, **10**, No. 12: 4759 (2020); https://doi.org/10.1007/s13204-020-01299-w

54. S.S. Stavitskaya, T.I. Mironyuk, N.T. Kartel, and V.V. Strelko, Sorption char-

acteristics of "food fibers" in secondary products of processing of vegetable raw materials, *Russ. J. Appl. Chem.*, **74**, No. 4: 592 (2001);
https://doi.org/10.1023/A:1012706531317

55. V.M. Gun'ko, V.V. Turov, T.V. Krupska, and E.M. Pakhlov, Behavior of water and methane bound to hydrophilic and hydrophobic nanosilicas and their mixture, *Chem. Phys. Lett.*, **690**: 25 (2017);
https://doi.org/10.1016/j.cplett.2017.10.039

56. O.I. Zakutevskii, T.S. Psareva, V.V. Strelko, and N.T. Kartel', Sorption of U(VI) from aqueous solutions with carbon sorbents, *Radiochemistry*, **49**, No. 1: 67 (2007);
https://doi.org/10.1134/S1066362207010110

57. I. Protsak, V.M. Gun'ko, V.V. Turov, T.V. Krupska, E.M. Pakhlov, D. Zhang, W. Dong, and Z. Le, Nanostructured polymethylsiloxane/fumed silica blends, *Materials*, **12**, No. 15: 2409 (2019);
https://doi.org/10.3390/ma12152409

58. M. Kartel and V. Galysh, New composite sorbents for caesium and strontium ions sorption, *Chem. J. Moldova*, **12**, No. 1: 37 (2017);
https://doi.org/10.19261/cjm.2017.401

59. V.M. Gun'ko, V.V. Turov, I.S. Protsak, T.V. Krupska, E.M. Pakhlov, and M.D. Tsapko, Effects of pre-adsorbed water on methane adsorption onto blends with hydrophobic and hydrophilic nanosilicas, *Colloids Surf. A*, **570**: 471(2019);
https://doi.org/10.1016/j.colsurfa.2019.03.056

60. V. Galysh, O. Sevastyanova, M. Kartel, M.E. Lindstrцm, and Y. Gornikov, Impact of ferrocyanide salts on the thermo-oxidative degradation of lignocellulosic sorbents, *J. Therm. Anal. Calorim.*, **128**, No. 2: 1019 (2017);
https://doi.org/10.1007/s10973-016-5984-7

61. V.V. Turov, V.M. Gun'ko, T.V. Krupska, M.V. Borysenko, and M.T. Kartel, Interfacial behavior of polar and nonpolar frozen/unfrozen liquids interacting with hydrophilic and hydrophobic nanosilicas alone and in blends, *J. Colloid Interface Sci.*, **588**: 70 (2021);
https://doi.org/10.1016/j.jcis.2020.12.065

62. M.T. Gabdullin, K.K. Khamitova, D.V. Ismailov, M.N. Sultangazina, D.S. Kerimbekov, S.S. Yegemova, A. Chernoshtan, and D.V. Schur, Use of nanostructured materials for the sorption of heavy metals ions, *IOP Conf. Ser.: Mat. Sci. Eng.*, **511**, No. 1: 012044 (2019);
https://doi.org/10.1088/1757-899X/511/1/012044

63. Yu.I. Sementsov, G.P. Prikhod'ko, A.V. Melezhik, T.A. Aleksyeyeva, and M.T. Kartel, Physicochemical properties and biocompatibility of polymer/carbon nanotubes composites, *Nanomaterials and Supramolecular Structures: Physics, Chemistry, and Applications*, p. 347 (2010);
https://doi.org/10.1007/978-90-481-2309-4_27

64. V.M. Gun'ko, T. Lupascu, T.V. Krupska, A.P. Golovan, E.M. Pakhlov, and V.V. Turov, Influence of tannin on aqueous layers at a surface of hydrophilic and hydrophobic nanosilicas, *Colloids Surf. A*, **531**: 9 (2017);
https://doi.org/10.1016/j.colsurfa.2017.07.084

65. K.K. Khamitova, B.A. Kayupov, S.S. Yegemova, M.T. Gabdullin, Kh.A. Abdullin, D.V. Ismailov, and D.S. Kerimbekov, The use of fullerenes as a biologically active molecule, *Int. J. Nanotechnol.*, **16**, Nos. 1–3: 100 (2019);
https://doi.org/10.1504/ijnt.2019.102396

66. V.M. Gun'ko, V.V. Turov, T.V. Krupska, and M.D. Tsapko, Interactions of human

serum albumin with doxorubicin in different media, *Chem. Phys.*, **483−484**: 26 (2017);
https://doi.org/10.1016/j.chemphys.2016.11.007

67. V.M. Gun'ko, V.V. Turov, T.V. Krupska, I.S. Protsak, M.V. Borysenko, and E.M. Pakhlov, Polymethylsiloxane alone and in composition with nanosilica under various conditions, *J. Colloid Interface Sci.*, **541**: 213 (2019);
https://doi.org/10.1016/j.jcis.2019.01.102

68. T.V. Krupska, A.A. Turova, V.M. Un'ko, and V.V. Turov, Influence of highly dispersed silica on physiological activity of yeast cells, *Biopolymers and Cell*, **25**, No. 4: 290 (2009);
https://doi.org/10.7124/bc.0007E8

69. L.M. Ushakova, K.I. Ivanenko, N.V. Sigareva, M.I. Terets, M.T. Kartel, and Yu.I. Sementsov, Influence of nanofiller on the structure and properties of macromolecular compounds, *Phys. Chem. Solid State*, **23**, No. 2: 394 (2022);
https://doi.org/10.15330/pcss.23.2.394-400

70. Y. Sementsov, G. Prikhod'ko, M. Kartel, M. Tsebrenko, T. Aleksyeyeva, and N. Ulyanchychi, Carbon nanotubes filled composite materials, *NATO Science for Peace and Security Series C: Environmental Security*, **2**: 183 (2011);
https://doi.org/10.1007/978-94-007-0899-0_16

71. E. Harea, R. Stoček, L. Storozhuk, Y. Sementsov, and N. Kartel, Study of tribological properties of natural rubber containing carbon nanotubes and carbon black as hybrid fillers, *Appl. Nanosci.*, **9**, No. 5: 899 (2019);
https://doi.org/10.1007/s13204-018-0797-6

72. V.M. Gun'ko, V.V. Turov, I. Protsak, T.V. Krupska, E.M. Pakhlov, and D. Zhang, Interfacial phenomena in composites with nanostructured succinic acid bound to hydrophilic and hydrophobic nanosilicas, *Colloids Interface Sci. Commun.*, **35**: 100251 (2020);
https://doi.org/10.1016/j.colcom.2020.100251

73. S. Tkachenko, D. Brodnikovskyi, J. Cizek, P. Komarov, Ye. Brodnikovskyi, Ya. Tymoshenko, S. Csaki, M. Pinchuk, O. Vasylyev, L. Čelko, M. Gadzyra, and T. Chraska, Novel Ti−Si−C composites for SOFC interconnect materials: Production optimization, *Ceram. Int.*, **48**, No. 19 (Pt. A): 27785 (2022);
https://doi.org/10.1016/j.ceramint.2022.06.081

74. V. Podhurska, D. Brodnikovskyi, B. Vasyliv, M. Gadzyra, S. Tkachenko, L. Čelko, O. Ostash, I. Brodnikovska, Ye. Brodnikovskyi, and O. Vasylyev, *Ti−Si−C in-situ Composite as a Potential Material for Lightweight SOFC Interconnects: Promising Materials and Processes in Applied Electrochemistry*, Monograph (Kyiv: KNUTD: 2020) p. 54;
https://er.knutd.edu.ua/handle/123456789/17000

75. Y. Brodnikovskyi, N. McDonald, I. Polishko, D. Brodnikovskyi, I. Brodnikovska, M. Brychevskyi, L. Kovalenko, O. Vasylyev, A. Belous, and R. Steinberger-Wilckens, Properties of 10Sc1CeSZ-3.5YSZ(33-, 40-, 50-wt.%) composite ceramics for SOFC application, *Mater. Today: Proc.*, **6**, Pt. 2: 26 (2019);
https://doi.org/10.1016/j.matpr.2018.10.071

76. I. Polishko, S. Ivanchenko, R. Horda, Ye. Brodnikovskyi, N. Lysunenko, and L. Kovalenko, Tape casted SOFC based on Ukrainian 8YSZ powder, *Mater. Today: Proc.*, **6**, Pt. 2: 237 (2019);
https://doi.org/10.1016/j.matpr.2018.10.100

77. A.F. Savenko, V.A. Bogolepov, K.A. Meleshevich, S.Yu. Zaginaichenko, M.V. Lototsky, V.K. Pishuk, L.O. Teslenko, and V.V. Skorokhod, Structural and methodical features of the installation for investigations of hydrogen-sorption cha-

racteristics of carbon nanomaterials and their composites, *NATO Security through Science Series A: Chemistry and Biology* (Dordrecht: Springer: 2007) p. 365; https://doi.org/10.1007/978-1-4020-5514-0_47

78. D.V. Schur, S. Zaginaichenko, and T.N. Veziroglu, Peculiarities of hydrogenation of pentatomic carbon molecules in the frame of fullerene molecule C_{60}, *Int. J. Hydrogen Energy*, **33**, No. 13: 3330 (2008); https://doi.org/https://doi.org/10.1016/j.ijhydene.2008.03.064

79. D.V. Schur, M.T. Gabdullin, S.Yu. Zaginaichenko, T.N. Veziroglu, M.V. Lototsky, V.A. Bogolepov, and A.F. Savenko, Experimental set-up for investigations of hydrogen-sorption characteristics of carbon nanomaterials, *Int. J. Hydrogen Energy*, **41**, No. 1: 401 (2016); https://doi.org/10.1016/j.ijhydene.2015.08.087

80. A.M. Lakhnik, I.M. Kirian, and A.D. Rud, The Mg/MAX-phase composite for hydrogen storage, *Int. J. Hydrogen Energy*, **47**, No. 11: 7274 (2022); https://doi.org/10.1016/j.ijhydene.2021.02.081

81. D.V. Schur, S.Y. Zaginaichenko, A.F. Savenko, V.A. Bogolepov, N.S. Anikina, A.D. Zolotarenko, Z.A. Matysina, T.N. Veziroglu, and N.E. Skryabina, Hydrogenation of fullerite C_{60} in gaseous phase, *NATO Science for Peace and Security Series C: Environmental Security* (Dordrecht: Springer: 2011) p. 87; https://doi.org/10.1007/978-94-007-0899-0_7

82. V.A. Bogolepov, A. Veziroglu, S.Y. Zaginaichenko, A.F. Savenko, and K.A. Meleshevich, Selection of the hydrogen-sorbing material for hydrogen accumulators, *Int. J. Hydrogen Energy*, **41**, No. 3: 1811 (2016); https://doi.org/10.1016/j.ijhydene.2015.10.011

83. D.V. Schur, M.T. Gabdullin, D.V. Shchur, S.Y. Zaginaichenko, A. Veziroglu, T.N. Veziroglu, N.A. Gavrylyuk, A.D. Zolotarenko, M.T. Gabdullin, T.S. Ramazanov, A.D. Zolotarenko, and A.D. Zolotarenko, Prospects of producing hydrogen-ammonia fuel based on lithium aluminum amide, *Rus. Phys. J.*, **64**, No. 1: 89 (2021); https://doi.org/10.1007/s11182-021-02304-7

84. Z.A. Matysina and D.V. Schur, Phase transformations $\alpha \to \beta \to \gamma \to \delta \to \varepsilon$ in titanium hydride TiH_x with increase in hydrogen concentration, *Rus. Phys. J.*, **44**, No. 11: 1237 (2001); https://doi.org/10.1023/A:1015318110874

85. V.I. Trefilov, D.V. Schur, V.K. Pishuk, S.Yu. Zaginaichenko, A.V. Choba, and N.R. Nagornaya, The solar furnaces for scientific and technological investigation, *Renewable Energy*, **16**, Nos. 1−4: 757 (1999); https://doi.org/10.1016/S0960-1481(98)00273-0

86. D.V. Schur, A.A. Lyashenko, V.M. Adejev, V.B. Voitovich, and S.Yu. Zaginaichenko, Niobium as a construction material for a hydrogen energy system, *Int. J. Hydrogen Energy*, **20**, No. 5: 405 (1995); https://doi.org/10.1016/0360-3199(94)00077-D

87. D.V. Schur, V.A. Lavrenko, V.M. Adejev, and I.E. Kirjakova, Studies of the hydride formation mechanism in metals, *Int. J. Hydrogen Energy*, **19**, No. 3: 265 (1994); https://doi.org/10.1016/0360-3199(94)90096-5

88. Z.A. Matysina, N.A. Gavrylyuk, M. Kartel, A. Veziroglu, T.N. Veziroglu, A.P. Pomytkin, D.V. Schur, T.S. Ramazanov, M.T. Gabdullin, A.D. Zolotarenko, A.D. Zolotarenko, and N.A. Shvachko, Hydrogen sorption properties of new magnesium intermetallic compounds with $MgSnCu_4$ type structure, *Int. J. Hydrogen Energy*, **46**, No. 50: 25520 (2021);

https://doi.org/10.1016/j.ijhydene.2021.05.069

89. Z.A. Matysina, O.S. Pogorelova, S.Yu. Zaginaichenko, and D.V. Schur, The surface energy of crystalline CuZn and FeAl alloys, *J. Phys. Chem. Sol.*, **56**, No. 1: 9 (1995);
https://doi.org/10.1016/0022-3697(94)00106-5

90. A.D. Rud, U. Schmidt, G.M. Zelinska, A.M. Lakhnik, G.Ya. Kolbasov, and M.O. Danilov, Atomic structure and hydrogen storage properties of amorphous−quasicrystalline Zr−Cu−Ni−Al melt-spun ribbons, *J. Non-Cryst. Sol.*, **353**, Nos. 32−40: 3434 (2007);
https://doi.org/10.1016/j.jnoncrysol.2007.05.095

91. Z.A. Matysina, S.Yu. Zaginaichenko, and D.V. Schur, Hydrogen solubility in alloys under pressure, *Int. J. Hydrogen Energy*, **21**, Nos. 11−12: 1085 (1996);
https://doi.org/10.1016/S0360-3199(96)00050-X

92. D.V. Schur, S.Yu. Zaginaichenko, Z.A. Matysina, I. Smityukh, and V.K. Pishuk, Hydrogen in lanthan−nickel storage alloys, *J. Alloys Comp.*, **330−332**: 70 (2002);
https://doi.org/10.1016/S0925-8388(01)01661-9

93. Yu.M. Lytvynenko and D.V. Schur, Utilization the concentrated solar energy for process of deformation of sheet metal, *Renewable Energy*, **16**, Nos. 1−4: 753 (1999);
https://doi.org/10.1016/S0960-1481(98)00272-9

94. Z.A. Matysina, S.Y. Zaginaichenko, D.V. Shchur, M.T. Gabdullin, Sorption properties of iron−magnesium and nickel−magnesium Mg_2FeH_6 and Mg_2NiH_4 hydrides, *Rus. Phys. J.*, **59**, No. 2: 177 (2016);
https://doi.org/10.1007/s11182-016-0757-0

95. A.D. Rud, U. Schmidt, G.M. Zelinska, A.M. Lakhnik, A.E.Perekos, G.Ya. Kolbasov, and M.O. Danilov, Peculiarities of structural state and hydrogen storage properties of Ti−Zr−Ni based intermetallic compounds, *J. Alloys Comp.*, **404−406**: 515 (2005);
https://doi.org/10.1016/j.jallcom.2004.12.174

96. S.Y. Zaginaichenko, Z.A. Matysina, L.O. Teslenko, and A. Veziroglu, The structural vacancies in palladium hydride. Phase diagram, *Int. J. Hydrogen Energy*, **36**, No. 1: 1152 (2011);
https://doi.org/10.1016/j.ijhydene.2010.06.088

97. S.Y. Zaginaichenko, D.A. Zaritskii, D.V. Schur, Z.A. Matysina, T.N. Veziroglu, and L.I. Kopylova, Theoretical study of hydrogen-sorption properties of lithium and magnesium borocarbides, *Int. J. Hydrogen Energy*, **40**, No. 24: 7644 (2015);
https://doi.org/10.1016/j.ijhydene.2015.01.089

98. Z.A. Matysina, S.Y. Zaginaichenko, and D.V. Schur, Hydrogen-sorption properties of magnesium and its intermetallics with Ca_7Ge-type structure, *Phys. Met. Metallogr.*, **114**, No. 4: 308 (2013);
https://doi.org/10.1134/S0031918X13010079

99. S.A. Tikhotskii, I.V. Fokin, and D.V. Schur, Traveltime seismic tomography with adaptive wavelet parameterization, *Izv. Phys. Solid Earth*, **47**, No. 4: 327 (2011);
https://doi.org/10.1134/S1069351311030062

100. N.S. Kurnakov, *Introduction to Physicochemical Analysis* (Leningrad: Academy of Sciences of the USSR: 1940), p. 564.

101. C. Smithells, *Gases and Metals* (Leningrad: Metallurgizdat: 1940), p. 228.

102. L.S. Darken and P.V. Guppy, *Physical Chemistry of Metals* (Moskva: Metal-

lurgizdat: 1960), p. 582.
103. V.B. Vyhodets, V.A. Goltsov, and P.V. Geld, *Physics of Metals and Metallography*, **26**: 933 (1968).
104. V.A. Goltsov, V.B. Vyhodets, P.V. Geld, and T.A. Krylov, *Physics of Metals and Metallography*, **30**: 657 (1970).
105. V.B. Vyhodets, V.A. Goltsov, and P.V. Geld, *Uspekhi Fiz. Nauk*, **15**: 107 (1970).
106. V.B. Vyhodets, V.A. Goltsov, and P.V. Geld, *Solid State Physics*, **12**: 2692 (1970).
107. A.A. Popov, *Problems of Metallurgy and Heat Treatment* (Moskva: Mashgiz: 1960).
108. I.I. Kornilov, *Proceedings of the Academy of Sciences of the USSR. Department of Chemical Sciences*, **4**: 337 (1947).
109. H. Bŭckle, *Rev. Met.*, **54**: 9 (1957).
110. I.A. Zelenkov and E.N. Martynchuk, *News of the Academy of Sciences of the Ukrainian SSR: Metallophysics*, vol. **50** (Kyiv: 1974).
111. E. Borelius, *Ann. d. Physic.*, **83**: 121 (1927);
     https://doi.org/10.1515/juru.1927.1927.4.121
112. L. Vegard, *Zeit. f. Pliysik*, **5**: 17 (1921).
113. L. Vegard, *Zeit. f. Kristall*, **67**: 148 (1928);
     https://doi.org/10.1524/zkri.1928.67.1.148
114. D. Stockdale, *J. Inst. Metals*, **66**: 287 (1940).
115. E.O. Kirkendall, *Trans. AIME*, **147**: 104 (1942).
116. E.A. Owen, *J. Inst. Metals*, **73**: 471 (1947).
117. H. Axon and W. Hume-Rothery, *Proc. Roy. Soc. A*, **193**: 1 (1948).
118. G.V. Raynor, *Trans. Faraday. Soc.*, **45**: 698 (1949);
     https://doi.org/10.1039/tf9494500698
119. J. Friedel, *Phil. Mag.*, **46**, Iss. 7: 514 (1955);
     https://doi.org/10.1080/14786440508520587
120. J.D. Eshelby, *Solid State Physics*, **3**: 79 (1959).
121. B. Warren, B. Averbach and B.J. Roberts, *Appl. Phys.*, **22**: 1493 (1951).
122. A.I. Bradley and A.H. Jay, *Proc. Roy. Soc.*, **136**: 210 (1932);
     https://doi.org/10.1098/rspa.1932.0075
123. W. Gordy, *Phys. Rev.*, **69**: 604 (1946);
     https://doi.org/10.1103/PhysRev.69.604
124. S.A. Pogodin and V.I. Mikheev, *Izv. SFHA*, **14**: 283 (1941);
     https://doi.org/10.1292/jvms1928.14.5_283
125. V.G. Kuznetsov, *Izv. SFHA*, **16**: 232 (1946).
126. D.M. Sivertsen and M.E. Nicholson, *Structure and Properties of Solid Solutions: Metallurgy* (1964).
127. J. Nicholas, *Proc. Phys. Soc. A*, **66**: 201 (1953);
     https://doi.org/10.1088/0370-1298/66/3/301
128. K. Huang, *Proc. Roy. Soc. A*, **190**: 102 (1947);
     https://doi.org/10.1098/rspa.1947.0064
129. D.M. Sivertsen and M.E. Nicholson, *Structure and Properties of Solid Solutions: Metallurgy* (1955).
130. L. Landau and E. Lifshitz, *Statistical Physics* (Pergamon–Elsevier: 1980).
131. M.A. Krivoglaz, *Journal of Technical Physics*, **24**: 1077 (1954).
132. M.A. Krivoglaz, *Physics of Metals and Metal Science*, **1**: 393 (1955).
133. N.V. Ageev, *Journal of Inorganic Chemistry AN USSR*, **3**: 557 (1958).
134. V.A. Nemilov and T.A. Vidusova, *Institute of General and Inorganic Chemistry,*

USSR Academy of Sciences: News from the Platinum Sector, **17**: 11 (1940).

135. V.V. Ageev, *Chemistry of Metal Alloys (Publishing House of the Academy of Sciences of the USSR:* 1941), p. 122.

136. V.I. Mikheev, *Proceedings of the Academy of Sciences of the USSR*: *Department of Chemical Sciences*, **6**: 396 (1944).

137. B.K. Wulf, *Physics of Metals and Metallography*, **3**: 97 (1956).

138. V. Hume-Rothery and G.V. Raynor, *Structure of Metals and Alloys* (Moskva: Metallurgizdat: 1959), p. 391.

139. B.K. Vul'f, Ternary intermetallic compounds, *Russ. Chem. Rev.*, **29**, No. 6: 364 (1960); https://doi.org/10.1070/rc1960v029n06abeh001238

140. G.B. Boky, B.K. Wulf, and N.L. Smirnova, *Journal of Structural Chemistry (Publishing House of the USSR Academy of Sciences)*, **2**, No.1: 74 (1961).

141. G.V. Samsonov, *Powder Metallurgy (Publishing house of the Academy of Sciences of the USSR)*, **2**: 3 (1962).

142. B.K. Vul'f, *Triple Metallic Phases in Alloys* (Moskva: Metallurgy: 1964).

143. Z.A. Matysina and E.A. Matysina, *Uspekhi Fiz. Nauk*, **14**: 1643 (1969).

144. Z.A. Matysina, *Izvestiya vuzov SSSR: Fizika*, **10**: 93 (1971).

145. Z.A. Matysina and E.A. Matysina, *Uspekhi Fiz. Nauk*, **17**: 14 (1972).

146. Z.A. Matysina, *Uspekhi Fiz. Nauk*, **14**, No. 10: 1638 (1969).

147. Z.A. Matysina, *Uspekhi Fiz. Nauk*, **17**: 9 (1972).

148. Z.A. Matysina and A.A. Smirnov, *Problems of Physics of Metals and Metallurgy*, **19**: 136 (1964).

149. Z.A. Matysina and A.A. Smirnov, *Problems of Physics of Metals and Metallurgy*, **19**: 136 (1964).

150. Z.A. Matysina, E.A. Matysina, and A.L. Chikarenko, *Mechanism and Kinetics of Crystallization* (Minsk: 1973).

151. V.I. Ryzhkov and A.A. Smirnov, *Physics and Mathematics Journal*, **18**: 670 (1964).

152. A.K. Buzzard, V.I. Ryzhkov, and A.A. Smirnov, *Metallofizika*, **3**: 22 (1965).

153. A.K. Kanyuka and A.A. Smirnov, *Uspekhi Fiz. Nauk*, **14**: 1626 (1969).

154. V.I. Ryzhkov, *Reports of the Academy of Sciences of the Ukrainian SSR*, No. 3: 277 (1970).

155. V.A. Goltsov, P.V. Geld, Yu.P. Simakov, M.M. Steinberg, and V.A. Native, *Diffusion Processes in Metals*, **17**: 92 (1969).

156. T.M. Radchenko, Pressure effect on order–disorder phase transformation temperature in $L1_2$- and $D0_{19}$-type superstructures, *Metallofiz. Noveishie Tekhnol.*, **30**, Spec. Iss.: 195 (2008).

157. T.M. Radchenko and V.A. Tatarenko, Fe–Ni alloys at high pressures and temperatures: statistical thermodynamics and kinetics of the $L1_2$ or $D0_{19}$ atomic order, *Usp. Fiz. Met.*, **9**, No. 1: 1 (2008); https://doi.org/10.15407/ufm.09.01.001

158. V.A. Tatarenko and T.M. Radchenko, Direct and indirect methods of the analysis of interatomic interaction and kinetics of a relaxation of the short-range order in close-packed substitutional (interstitial) solid solutions, *Usp. Fiz. Met.*, **3**, No. 2: 111 (2002); https://doi.org/10.15407/ufm.03.02.111

159. S.M. Bokoch, M.P. Kulish, T.M. Radchenko, and V.A. Tatarenko, Kinetics of short-range ordering of substitutional solid solutions (according to data on a scattering of various kinds of waves). I. Microscopic parameters of migration of atoms within f.c.c.-Ni–Mo in Fourier-representation, *Metallofiz. Noveishie Tekhnol.*, **26**, No. 3: 387 (2004).

160. S.M. Bokoch, M.P. Kulish, V.A. Tatarenko, and T.M. Radchenko, Kinetics of

short-range ordering of substitutional solid solutions (according to data on a scattering of various kinds of waves). II. Parameters of atomic microdiffusion within f.c.c.-Ni−Mo, *Metallofiz. Noveishie Tekhnol.*, **26**, No. 4: 541 (2004)

161. V.A. Tatarenko and T.M. Radchenko, Diffusive relaxation of short-range order parameters and the time evolution of diffuse radiation scattering in solid solutions, *Defect Diffus. Forum*, **194−199**, Pt. 1: 183 (2001);
https://doi.org/10.4028/www.scientific.net/DDF.194-199.183

162. T.M. Radchenko and V.A. Tatarenko, Comments concerning parameters of the short-range order evolution determined from the data on kinetics of a heat-capacity relaxation for Lu−H alloy, *Hydrogen Materials Science and Chemistry of Carbon Nanomaterials. NATO Security through Science Series A: Chemistry and Biology* (Eds. T.N. Veziroglu, S.Yu. Zaginaichenko, D.V. Schur, B. Baranowski, A.P. Shpak, V.V. Skorokhod, and A. Kale) (Dordrecht: Springer: 2007), p. 229;
https://doi.org/10.1007/978-1-4020-5514-0_28

163. V.A. Tatarenko, S.M. Bokoch, V.M. Nadutov, T.M. Radchenko, and Y.B. Park, Semi-empirical parameterization of interatomic interactions and kinetics of the atomic ordering in Ni−Fe−C permalloys and elinvars, *Defect Diffus. Forum*, **280−281**: 29 (2008);
https://doi.org/10.4028/www.scientific.net/DDF.280-281.29

164. T.M. Radchenko, V.A. Tatarenko, H. Zapolsky, and D. Blavette, Statistical-thermodynamic description of the order−disorder transformation of $D0_{19}$-type phase in Ti−Al alloy, *J. Alloys Compd.*, **452**, No. 1: 122 (2008);
https://doi.org/10.1016/j.jallcom.2006.12.149

165. T.M. Radchenko, V.A. Tatarenko, and H. Zapolsky, Statistical-thermodynamics and ordering kinetics of $D0_{19}$-type phase: application of the models for h.c.p.-Ti−Al alloy, *Solid State Phenom.*, **138**: 283 (2008);
https://doi.org/10.4028/www.scientific.net/SSP.138.283

166. V.A. Tatarenko and T.M. Radchenko, The application of radiation diffuse scattering to the calculation of phase diagrams of f.c.c. substitutional alloys, *Intermetallics*, **11**, Nos. 11−12: 1319 (2003);
https://doi.org/10.1016/S0966-9795(03)00174-2

167. T.M. Radchenko and V.A. Tatarenko, Atomic-ordering kinetics and diffusivities in Ni−Fe permalloy, *Defect Diffus. Forum*, **273−276**: 525 (2008);
https://doi.org/10.4028/www.scientific.net/DDF.273-276.525

168. T.M. Radchenko, O.S. Gatsenko, V.V. Lizunov, and V.A. Tatarenko, Martensitic α''-$Fe_{16}N_2$-type phase of non-stoichiometric composition: current status of research and microscopic statistical-thermodynamic model, *Prog. Phys. Met.*, **21**, No. 4: 580 (2020);
https://doi.org/10.15407/ufm.21.04.580

169. T.M. Radchenko and V.A. Tatarenko, Kinetics of the orientational long-range ordering of interstitial hydrogen atoms in metals having hexagonal close-packed structure, *Carbon Nanomaterials in Clean Energy Hydrogen Systems. NATO Science for Peace and Security Series C: Environmental Security* (Eds. B. Baranowsky, S.Y. Zaginaichenko, D.V. Schur, V.V. Skorokhod, and A. Veziroglu) (Springer Science + Business Media B.V.: 2008), p. 489;
https://doi.org/10.1007/978-1-4020-8898-8_62

170. I.M. Melnyk, T.M. Radchenko, and V.A. Tatarenko, Semi-empirical parameterization of interatomic interactions, which is based on statistical-thermodynamic analysis of data on phase equilibriums in b.c.c.-Fe−Co alloy. I. Primary ordering, Metallofiz. Noveishie Tekhnol., 32, No. 9: 1191 (2010).

Ан.Д. Золотаренко[1,2] , *Ол.Д. Золотаренко*[1,2], *З.А. Матисіна*[1],
Н.А. Швачко[1,3], *Н.Є. Аханова*[4,5], *М. Уалханова*[5], *Д.В. Щур*[1,6],
М.Т. Габдуллін[4], *Ю.І. Жирко*[6], *Ю.М. Солонін*[1], *В.В. Лобанов*[2],
Д.В Ісмаїлов[5,7], *О.Д. Золотаренко*[1], *І.В. Загорулько*[8]

[1] Інститут проблем матеріалознавства ім. І.М. Францевича НАН України,
   вул. Омеляна Пріцака, 3, 03142 Київ, Україна
[2] Інститут хімії поверхні ім. О.О. Чуйка НАН України,
   вул. Генерала Наумова, 17, 03164 Київ, Україна
[3] Київський національний університет будівництва і архітектури,
   просп. Повітрофлотський, 31, 03037 Київ, Україна
[4] Казахстансько-британський технічний університет,
   вул. Толе бі, 59, 050040 Алмати, Казахстан
[5] Казахський національний університет ім. Аль-Фарабі,
   просп. Аль-Фарабі, 71, 050040 Алмати, Казахстан
[6] Інститут прикладної фізики НАН України,
   вул. Петропавлівська, 58, 40000 Суми, Україна
[7] НАТ «Казахський національний дослідницький технічний університет
   імені К.І. Сатбаєва», вул. Сатбаєва, 22, 050013 Алмати, Казахстан
[8] Інститут металофізики ім. Г.В. Курдюмова НАН України,
   бульв. Академіка Вернадського, 36, 03142 Київ, Україна

ПРО РОЗЧИННІСТЬ ГІДРОҐЕНУ У МЕТАЛАХ І СТОПАХ

Оглянуто та проаналізовано чинники впливу на розчинність атомів втілення (H) у металевих стопах. Розглянуто електронну структуру й атомове впорядкування стопів типу *AB*, а також методи розрахунку розчинности для упорядковних кубічних стопів з октаедричними порами втілення. Вивчено параметри атомів втілення, що уможливлюють прогноз зменшення або збільшення розчинности, коли головну роль відіграє впорядкування системи. Встановлено параметри статичного розподілу атомів. Розглянуто відносну розчинність як функцію параметра далекого порядку (η) та вплив об'ємних ефектів на величину цього параметра. Розглянуто наступні системи: Fe–Ni, Au–Cu, Pd–Au, Fe–Cr, Ti–Al, Cu–Zn, Ag–Zn, Fe–Al, Au–Ag, Fe–V, Pd–Pt, Ni–Mn, Ni–Fe, Cu–Au, Cu–Pd, Pd–Nb, Pd–Ag, а також трикомпонентні стопи. Показано, що шляхом введення домішок у стоп можна значною мірою змінити його фізико-механічні, електричні, магнетні й інші властивості.

Ключові слова: метали, стопи, атоми втілення, розчинність, упорядкування, об'ємноцентрована кубічна (ОЦК) структура, гранецентрована кубічна (ГЦК) структура, молекулярно-кінетична теорія.